JCAMECH

Vol. 48, No. 1, June 2017, pp 65-74
DOI: 10.22059/jcamech.2017.232031.138

Parametric study of a viscoelastic RANS turbulence model in the fully developed channel flow

Saber Azad, Hamed Amiri Moghadam, Alireza Riasi∗, Hossien Mahmoodi darian

School of Mechanical Engineering, College of Engineering, University of Tehran

Received: 26 Apr. 2017, Accepted: 19 June. 2017

Abstract

One of the newest of viscoelastic RANS turbulence models for drag reducing channel flow with polymer additives is studied in different flow and rheological properties. In this model, finitely extensible nonlinear elastic-Peterlin (FENE-P) constitutive model is used to describe the viscoelastic effect of polymer solution and turbulence model is developed in the $k-\epsilon-\overline{v^2}-f$ framework. The geometry in this study is two-dimensional channel flow and finite volume method (FVM) with a non-uniform collocated mesh is used to solve the momentum and constitutive equations. In order to evaluate this turbulence model, several cases with different parameters such as Reynolds numbers, Weissenberg number, maximum polymer extensibility and concentration of polymer are simulated and assessed against direct numerical simulation (DNS) data. The velocity profiles, shear stress profiles and the percentage of friction drag reduction predicted by this turbulence model are in good agreement with DNS data at moderate to high Reynolds numbers. However, in low Reynolds numbers, the results of model are reliable only for low L^2 value. Moreover, in case of high concentration of polymer, the accuracy of the model is lost.

Keywords: Drag Reduction, FENE-P Fluid, Polymer Additives, Turbulent Flow, Viscoelastic RANS Model

1. Introduction

It is known that the addition of small amounts of polymer additives can reduce friction drag in wall-bounded turbulent flows. According to some experiments, very small amounts of polymers are sufficient to reduce friction drag up to 80% [1]. Also, it has been known experimentally that the drag reduction (DR) occurs in turbulent flows when the ratio of polymer time scale to the flow time scale in the near-wall turbulence, defined as the wall-shear Weissenberg number, is of order unity [2].

Numerical simulation of dilute polymer solutions has been a great field of study for many researchers. In order to study these fluids, viscoelastic models like Oldroyd-B and FENE-P (finitely extensible nonlinear elastic-Peterlin) are often used. The FENE-P model is widely used in literature because it accounts for the effect of chain extensibility [2]. Some of the researchers used direct numerical simulation (DNS) to identify complex mechanism of turbulent drag reduction (DR) in polymer solutions [3-7]. Because DNS are usually costly and impractical to be used in engineering applications, another group of researchers developed Reynolds-averaged Navier–Stokes (RANS)

∗ Corresponding Author. Tel.: +98 21 611 19918
Email Address: ariasi@ut.ac.ir

models [8-11] and large eddy simulation method [12] based on the DNS results.

Pinho [8] is one of the earliest researchers who developed the k-ε turbulence model based on the modified version of Generalized Newtonian Fluid constitutive equation (GNF) for drag reducing fluids. Also for the FENE-P fluids, Pinho and coworkers [9, 10] used k-ε and k-ω model to simulate fully turbulent channel flow of dilute polymer solutions. In addition to the complexity, these models are not able to predict accurately flow parameters in the high drag reduction (HDR) regime. Based on the FENE-P constitutive equation, Iaccarino et al. [11] modified $k-\epsilon-\overline{v^2}-f$ model which was firstly introduced by Durbin [13] for Newtonian fluids. In order to account for the effect of viscoelasticity in the turbulence model, they introduced a new turbulent polymer viscosity. In this model simple closures for non-linear terms are proposed and although in several cases in both moderate and high drag reduction regimes it was able to accurately predict amount of drag reduction, some of flow parameters such as polymer shear stress and turbulent kinetic energy was not in agreement with DNS results. Masoudian et al. [14] proposed a similar model to the Iaccarino's one [11] based on the $k-\epsilon-\overline{v^2}-f$ turbulence model with new closures. Due to use of several precise closures for the nonlinear turbulent terms, results of this model were in better agreement with DNS data than that of Iaccarino et al. [11]. Masoudian et al. [14] examined their model with several cases which all were with low polymer concentration at moderate to high Reynolds numbers. It is important to determine the ability of this model in prediction of the flow parameters in all conditions such as higher polymer concentration and lower Reynolds numbers. The object of the present study is to investigate the ability of Mosudian et al. [14] model in prediction of DR value, velocity and shear stress profiles in fully turbulent channel flow with different flow and rheological parameters. In order to implement new turbulence model developed by Masoudian et al. [14], we use an open-source CFD tool, OpenFOAM (Open Source Field Operation and Manipulation) package. After code validation, we have assessed performance of Masoudian et al. [14] model against DNS data in different cases.

The paper is organized as follows: Section 2 presents governing equations of turbulence model of Masoudian et al. [14] for FENE-P fluids. Numerical methods are briefly introduced in Section 3. Results and discussion are given in Section 4 which is divided into grid study, code validation and performance of Masoudian et al.'s turbulence model [14] at low Reynolds number and in high polymer concentration. Conclusion is given in Section 5.

2. Governing equations

The rheological description of dilute polymer solutions in Masoudian et al.'s model [14] is based on FENE-P constitutive equation. The momentum equation for an incompressible viscoelastic flow is [11, 14]:

$$\rho\frac{\partial u_i}{\partial t}+\rho u_j\frac{\partial u_i}{\partial x_j}=-\frac{\partial p}{\partial x_i}+\rho\frac{\partial}{\partial x_j}\left[\nu_s\frac{\partial u_i}{\partial x_j}\right]+\frac{\partial \tau_{ij}^p}{\partial x_j} \quad (1)$$

In the above equation, ρ and ν_s represent density and viscosity of the solvent and u_i and p are the velocity components and pressure, respectively. The second and third terms of the right hand side of Eq. (1) are viscous and polymer stresses. The polymer stress definition based on the FENE-P model is as follows [14, 15]:

$$\tau_{ij}^p=\frac{\eta_p}{\lambda}(c_{ij}f(c_{kk})-\delta_{ij}) \quad (2)$$

Where $f(c_{kk})$ is the Peterlin function defined as [14]:

$$f(c_{kk})=\frac{L^2-3}{L^2-c_{kk}} \quad (3)$$

In the above equations, η_p, λ and L^2 represent polymer intrinsic viscosity, relaxation time and maximum extension of the polymer chains, respectively. The other variable which appears in Eq.

(2) is conformation tensor c_{ij}. The trace of conformation tensor c_{kk} represents the elongation of the polymer chains and it is normalized with respect to the characteristic polymer length in the equilibrium no-flow state. The conformation tensor obeys a hyperbolic differential equation of the form [14]:

$$\frac{\partial c_{ij}}{\partial t}+u_k\frac{\partial c_{ij}}{\partial x_k}-c_{jk}\frac{\partial u_i}{\partial x_k}-c_{ik}\frac{\partial u_j}{\partial x_k}=\frac{1}{\lambda}(\delta_{ij}-f(c_{kk})c_{ij}) \quad (1)$$

By Reynolds averaging the instantaneous equations, the Reynolds-averaged momentum equation becomes [11, 14]:

$$\rho\frac{\partial U_i}{\partial t}+\rho U_j\frac{\partial U_i}{\partial x_j}=-\frac{\partial P}{\partial x_i}+\rho\frac{\partial}{\partial x_j}\left[(\nu_s+\nu_t)\frac{\partial U_i}{\partial x_j}\right]+\frac{\partial \overline{\tau_{ij}^p}}{\partial x_j} \quad (2)$$

Where U_i represent the mean velocity components and ν_t is the turbulent viscosity. In addition to ν_t, mean polymer stress in Eq. (4) should be defined. For this purpose Masoudian et al. [14] used turbulent polymer viscosity concept which was introduced

previously by Iaccarino et al. [11]. According to Masoudian et al.'s model mean polymer stress is defined as [14]:

$$\overline{\tau_{ij}^{p}} = \nu_{t,p}\frac{\partial U_i}{\partial x_j} \tag{3}$$

In the equation above, $\nu_{t,p}$ is the turbulent polymer viscosity. In order to define ν_t Masoudian et al. [14] modified the $k-\epsilon-\overline{v^2}-f$ model of Durbin [13] which was firstly proposed for Newtonian fluids. According to Masoudian et al.'s model [14], for fully-developed turbulent channel flow of viscoelastic fluids described by the FENE-P model, we need to solve just the trace of the mean conformation tensor (C_{kk}). To sum up, the Reynolds-averaged governing and the model equations of turbulent viscoelastic flow which was developed by Masoudian et al. [14] are given below:

$$\frac{\partial U_i}{\partial x_i} = 0 \tag{4}$$

$$\rho\frac{\partial U_i}{\partial t} + \rho U_j\frac{\partial U_i}{\partial x_j} = -\frac{\partial P}{\partial x_i} + \rho\frac{\partial}{\partial x_j}[(\nu_s+\nu_t+\nu_{t,p})\frac{\partial U_i}{\partial x_j}] \tag{5}$$

$$U_j\frac{\partial k}{\partial x_j} = P_k - \varepsilon + \frac{\partial}{\partial x_j}\left(\left(\nu_s+\frac{\nu_t}{\sigma_k}\right)\frac{\partial k}{\partial x_j}\right) - \varepsilon_p \tag{6}$$

$$U_j\frac{\partial \varepsilon}{\partial x_j} = \frac{C_{\varepsilon1}P_k - C_{\varepsilon2}\varepsilon}{T_t} + \frac{\partial}{\partial x_j}\left(\left(\nu_s+\frac{\nu_t}{\sigma_\varepsilon}\right)\frac{\partial \varepsilon}{\partial x_j}\right) - E_p \tag{7}$$

$$U_j\frac{\partial \overline{v^2}}{\partial x_j} = kf + \frac{\partial}{\partial x_j}\left(\left(\nu_s+\frac{\nu_t}{\sigma_k}\right)\frac{\partial \overline{v^2}}{\partial x_j}\right) - \frac{6\varepsilon}{k}\overline{v^2} - \varepsilon_{p,yy} \tag{8}$$

$$f - L_t^2\frac{\partial^2 f}{\partial x_j \partial x_j} = (C_1-1)\frac{\left(\frac{2}{3}-\frac{\overline{v^2}}{k}\right)}{T_t} + C_2\frac{P_k}{k} + 5\varepsilon\frac{\overline{v^2}}{k} \tag{9}$$

$$M_{kk} + NLT_{kk} + \frac{1}{\lambda}(3 - f(C_{kk})C_{kk}) + \kappa\frac{\partial}{\partial x_j}(\frac{\partial C_{kk}}{\partial x_j}) = 0 \tag{10}$$

In the above equations, k and $\overline{v^2}$ are turbulent kinetic energy and its wall normal component, ε is the dissipation rate of turbulent kinetic energy and f is the energy redistribution process that plays a crucial role in producing $\overline{v^2}$. In order to stabilize the numerical method, an artificial diffusivity (κ) is added to the trace of mean conformation tensor equation. The turbulent viscosity and the new turbulent polymer viscosity in the momentum equation (Eq. (8)) are defined as [14]:

$$\nu_t = C_\mu\overline{v^2}T_t \tag{11}$$

$$T_t = max(\frac{k}{\varepsilon}, 6\sqrt{\frac{\nu_s}{\varepsilon}}) \tag{12}$$

$$\nu_{t,p} = \frac{\nu_p}{f(C_{kk})} + a_1\sqrt{\frac{L^2}{Wi_{\tau0}}}f(C_{kk})\nu_t \tag{13}$$

$$Wi_{\tau o} = \frac{\lambda U_\tau^2}{\nu_o} \quad , \nu_o = \nu_p + \nu_s \tag{14}$$

The new source terms for FENE-P fluids in Eq. (9) to Eq. (13) are given below according to Masoudian et al.'s model [14]:

$$\varepsilon_p = \frac{\mu_p}{2\rho\lambda}f(C_{kk})NLT_{kk} \tag{15}$$

$$\varepsilon_{p,yy} = a_1a_3Lf(C_{kk})kf \tag{16}$$

$$E_p = \frac{C_{\varepsilon1}\varepsilon_p}{T_t} \tag{17}$$

$$M_{kk} = 2\left\{\frac{\lambda}{f(C_{kk})}\frac{\nu_{t,p}}{\nu_p}\left(\frac{dU}{dy}\right)^2\right\} \tag{18}$$

$$NLT_{kk} = a_2M_{kk}\frac{\nu_t}{\nu_o} \tag{19}$$

Where a_1, a_2 and a_3 are the model's constants. The length scale in diffusion term in Eq. (12) (for f equation) is defined with the following expression [14]:

$$L_t^2 = C_l^2max\{\frac{k^3}{\varepsilon^2}, C_\eta^2\sqrt{\frac{\nu^3}{\varepsilon}}\} \tag{20}$$

Where C_l and C_η are constant. Finally all the constants in the above equations are listed in Table 1 [14].

3. Numerical method

In the present study Finite Volume Method was used with a non-uniform collocated mesh. The height of the first mesh cell adjacent to the walls is set carefully in order to achieve $y^+ \sim 1$ at the walls. SIMPLE algorithm is adopted to solve the coupling of velocity and pressure equations. Second order schemes are used in order to discretize equations. Periodic boundary condition is set in the streamwise direction and no-slip boundary conditions are set at the bottom and top walls. Except ε and C_{kk}, all parameters are set to zero on the walls and the wall boundary conditions for these two parameters are defined as [11]:

$$\varepsilon = 2\nu_s\left(\frac{\partial\sqrt{k}}{\partial n}\right)^2 \tag{21}$$

$$\frac{\partial C_{kk}}{\partial n} = 0 \tag{22}$$

Where n represents the normal direction to the wall. As in earlier studies [5, 14], the value of the dimensionless artificial diffusivity based on the half channel height (h) and friction velocity (u_τ) is taken to be $\frac{\kappa}{hu_\tau} \sim$ O (10^{-2}) to achieve stable numerical integration and have no effect on the results. In this study we pursued the simulations up to a tolerance of 10^{-6} and results remain practically identical to those for lower tolerance of 10^{-5}.

4. Results and discussion

4.1. *Grid study*

The geometry in this study is a 2D channel with a height of 2h and length of 10h. The grid convergence study was performed by developing five different grids. The mesh independency analysis for the two cases (moderate and high drag reduction) is reported in Table 2 where N_y shows the number of nodes in the wall-normal direction and N_x shows the number of nodes in the streamwise direction. In Table 2 the error are calculated based on mesh M5 for both drag reduction value (DR) and normalized centerline velocity (u_c^+**)**. According to Table 2, although all errors are below 0.5%, the third grid is chosen as independent grid for better accuracy. Drag reduction in Table 2 is calculated by Eq. (26) [3]:

$$DR\% = \left(1 - \frac{C_{f,Vis}}{C_{f,new}}\right) \times 100 \tag{23}$$

Where subscripts of "vis" and "new" represent the viscoelastic and Newtonian fluids, respectively. It is important to mention that the friction coefficient for Newtonian and viscoelastic fluid are calculated at the same bulk Reynolds number (i.e. $Re_b = \frac{\rho 2hU_b}{\mu}$).

In above equation the friction coefficient is defined as [3]:

$$C_f = \frac{\tau_w}{\frac{1}{2}\rho U_b^2} \tag{24}$$

Where τ_w is the wall shear stress and U_b is the bulk velocity in the channel. For fully developed turbulent channel flow of Newtonian fluids the friction coefficient is given by Dean [16] as:

$$C_f = 0.073 Re_b^{-0.25} \tag{25}$$

Table 1-Coefficients of viscoelastic turbulence model developed by Masoudian et al. [14]

constant	C_μ	σ_k	σ_ε	$C_{\varepsilon 1}$	$C_{\varepsilon 2}$	C_1	C_2	C_l	C_η	a_1	a_2	a_3
value	0.22	1	1.3	$1.4(1 + 0.05\sqrt{\frac{k}{\overline{v^2}}})$	1.9	1.4	0.3	0.23	70	0.02	0.16	0.15

Table 2-Mesh independency analysis

Grid	$N_y * N_x$	DR1	Error (%)	u_c^+	Error (%)	DR2	Error (%)	u_c^+	Error (%)
M1	65*65	40.14	0.47	26.28	0.23	63.73	0.16	35.61	0.22
M2	99*99	40.20	0.32	26.28	0.23	63.75	0.12	35.63	0.14
M3	111*111	40.25	0.2	26.32	0.075	63.78	0.08	35.65	0.11
M4	144*144	40.26	0.17	26.33	0.038	63.82	0.016	35.68	0.03
M5	199*199	40.33	-	26.34	-	63.83	-	35.69	-

4.2. *Validation of code*

For fully turbulent channel flow of FENE-P fluids the flow and rheological properties is fully characterized by four dimensionless parameters: friction Reynolds number, friction Weissenberg number, ratio of solvent viscosity to total viscosity and maximum extension of the polymer chains. The first three numbers are defined as [14]:

$$Re_\tau = \frac{\rho u_\tau h}{\mu_0} \quad (26)$$

$$Wi_\tau = \frac{\rho \lambda u_\tau^2}{\mu_0} \quad (27)$$

$$\beta = \frac{\mu_s}{\mu_0} = \frac{\mu_s}{\mu_s + \mu_p} \quad (28)$$

Where h is the channel half height, λ is the relaxation time for viscoelastic solvent, u_τ is the wall shear stress velocity ($u_\tau = \sqrt{\frac{\tau_w}{\rho}}$) and μ_0 is the solution total viscosity at zero shear rate ($\mu_0 = \mu_s + \mu_p$). In order to benchmark our methodology, the numerical simulation results for two cases of fully-developed channel flow are presented and assessed against DNS data [5, 14] for velocity profile and wall shear stress. Flow and rheological parameters of these two cases are given in Table 3.

The normalized velocity profile of the current study and that of Masoudian et al. [14] for cases A1 and A2 are presented in Fig. 1. As shown in this figure, the prediction of velocity profile of the current study is in very good agreement with the results of Masoudian et al. [14] for both cases. Furthermore, according to Fig. 2, three components of normalized wall shear stress of case A1 (solvent, polymer and turbulence shear stress) are in good agreement with [14]. Overall, comparing the results of current study with that of Masoudian et al. [14] validates the developed code.

Table 3-Flow and rheological parameters of two cases for code validation [5, 14]

Case	Flow and Rheological properties				Drag reduction	
	Re_τ	β	Wi_τ	L^2	DNS	current study
A1	395	0.9	100	900	37	40
A2	395	0.9	100	14400	61	64

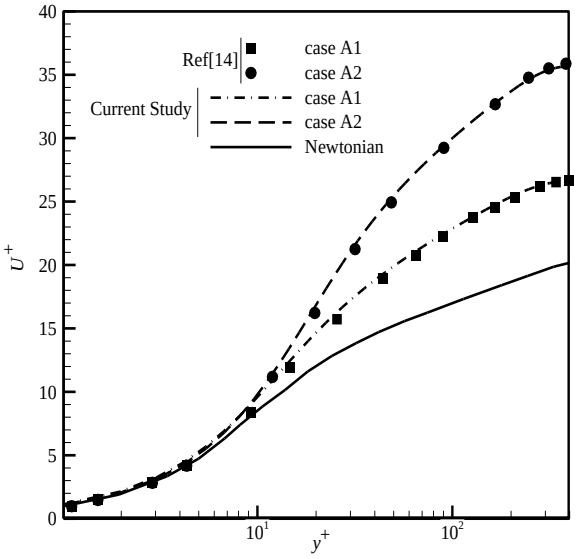

Figure 1-Normalized velocity profile of Ref [14] and current study for case A1 and A2

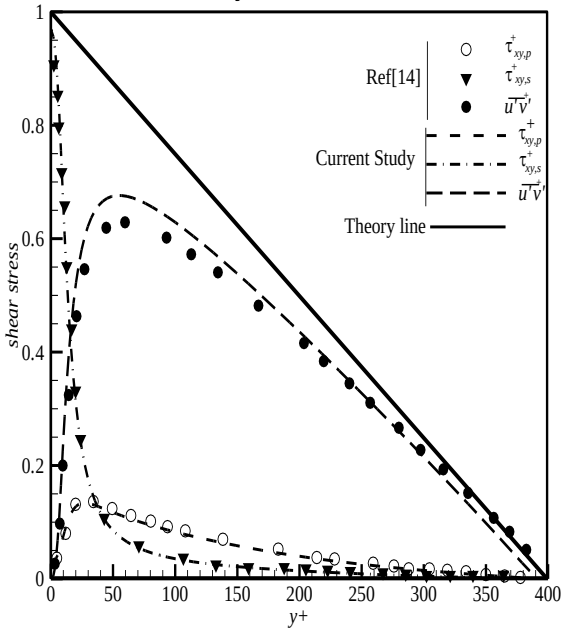

Figure 2-Normalized wall shear stress profile of Ref [14] and current study for case A1

4.3. *Prediction of the turbulence model at* $Re_\tau = 125$

In this section, we investigate the performance of viscoelastic turbulence model developed by Masoudian et al. [14] at several cases with $Re_\tau = 125$ and different L^2 and Weissenberg number values of Li et al. [5] which the rheological properties of these cases are summarized in Table 4.

Table 4- Comparison of drag reduction prediction at $\boldsymbol{Re_\tau = 125}$

Case	Rheological properties			Drag reduction	
	β	Wi_τ	L^2	DNS	Current study
B1	0.9	25	900	20	23
B2	0.9	25	3600	22	30
B3	0.9	25	14400	24	41
B4	0.9	50	900	31	28
B5	0.9	50	3600	43	35
B6	0.9	50	14400	51	39
B7	0.9	100	900	37	38
B8	0.9	100	3600	56	45
B9	0.9	100	14400	74	60

According to Table 4, in the cases with $L^2 = 900$, the amount of predicted drag reduction by Masoudian et al.'s turbulence model [14] are comparable with the DNS data at all Weissenberg numbers ($Wi_\tau = 25{,}50\ and\ 100$). However, by increasing L^2 from 900 to 3600, the difference between the drag reductions by Masoudian et al. [14] turbulence model and DNS data becomes more noticeable (around 8%). Moreover, the DR prediction at $L^2 = 14400$ are quite far away of the DNS results.

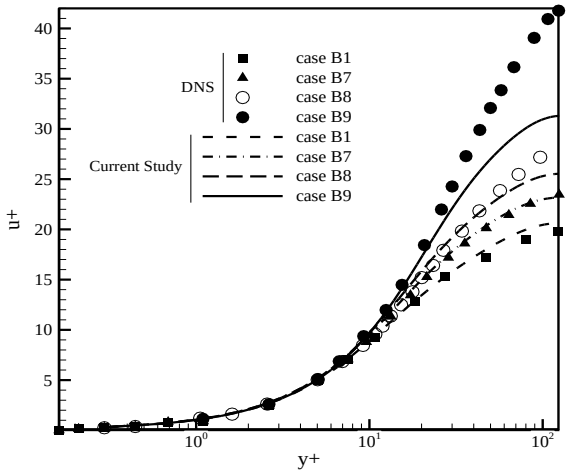

Figure 3- Normalized velocity profile of DNS data [5] and current study for case B1, B7, B8 and B9

Figure 3 shows the normalized velocity profile for cases B1, B7, B8 and B9. As shown in the figure, the velocity profile of case B1 and B7 have the minimum difference with DNS results as their amount of DR is fairly well predicted. But the predicted velocity profiles for case B9 is inconsistent with the DNS results as expected from the amount of DR prediction.

Among cases with available shear stress profile in Ref. [5], the result of case B8 has minimum difference in DR prediction. Therefore, in the Fig. 4 normalized wall shear stress for case B8 is compared with DNS data. According to this figure, although the trends of predicted wall shear stresses and the DNS data are completely similar, their values are different. Near the wall, polymer and viscous shear stress predictions are fairly well comparable with the DNS results however, by getting away from the wall, Masoudian et al.'s turbulence model [14] could not predict these shear stresses well. Furthermore, across the channel, turbulent shear stress values were predicted higher than the DNS results.

The results of this section demonstrate that in cases with low value of L^2, predictions of Masoudian et al.'s turbulence model [14] are acceptable. However, by increasing the value of L^2, although the trend of increasing DR value is similar to DNS data, the difference between their values could be quite significant especially at high Wi_τ.

4.4. *Prediction of the turbulence model at* $\boldsymbol{Re_\tau = 180}$

In this section, three cases with $Re_\tau = 180$ and different rheological parameters have been studied. The flow and rheological properties of these cases

and amount of DR predicted by current study are summarized in Table 5 [5]. According to these results, there is a good agreement between the DNS data and predictions by the current study in terms of DR value. Furthermore, as shown in Fig. 5 and Fig. 6 normalized velocity and shear stress profiles for these cases match fairly well with the DNS data even in cases with high value of L^2.

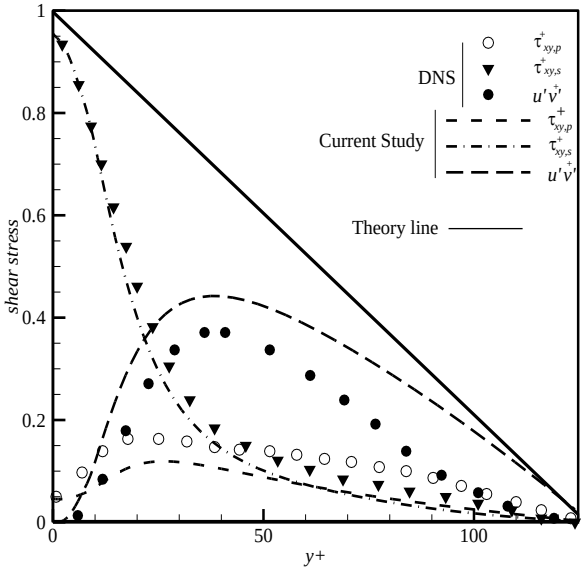

Figure 4- Normalized wall shear stress profile of DNS data [5] and current study for case B8

Table 5- Comparison of drag reduction prediction at $\boldsymbol{Re_\tau = 180}$

Case	Rheological properties			Drag reduction	
	β	Wi_τ	L^2	DNS	current study
C1	0.9	50	900	31	29
C2	0.9	100	900	37	41
C3	0.9	100	14400	61	64

Comparing the results of this section with section 4.3 shows by increasing the Reynolds number, the results of Masoudian et al.'s turbulence model [14] are better match with the DNS data [5] regardless of L^2.

4.5. *Results for lower β value*

Masoudian et al. [14] developed their viscoelastic turbulence model for $\beta = 0.9$ based on the DNS data. But it is important to examine the accuracy of this model for lower β values which represent higher concentration of polymers. For this purpose we have selected five different cases of Petasiniski et al. [3] which all have lower solvent to total solution viscosity ratio (lower β value). Flow and rheological properties of these cases are shown in Table 6.

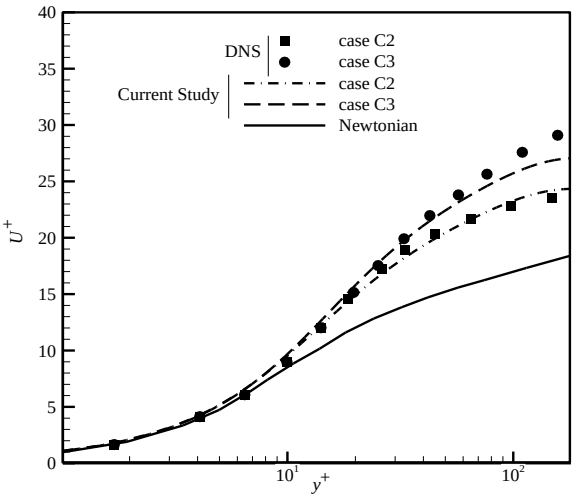

Figure 5-Normalized velocity profile of DNS data [5] and current study for case C2 and C3.

Based on Table 6, the DNS data demonstrates that by decreasing value of β or by increasing the value of L^2, the amount of drag reduction will increase. However, the result of D4, D1 and D5 (decreasing β) and D1 and D2 (increasing L^2) in Table 5, it is obvious that Masoudian et al.'s turbulence model [14] could not predict these trends. Furthermore, prediction of DR value is comparable with DNS data in just two cases, D1 and D4. Comparison of C1 in Table 5 with D2 in Table 6 also confirms that Masoudian et al.'s turbulence model [14] does not have an acceptable accuracy in prediction of DR value in high polymer to solvent viscosity ratio (low β value), and even accuracy of model is completely lost by decreasing β from 0.8 to 0.4 in case D5.

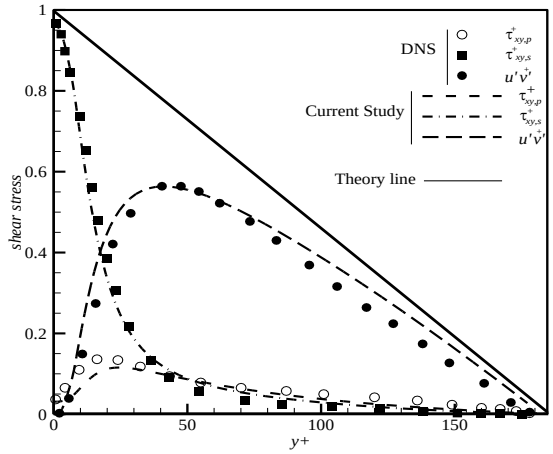

Figure 6-Normalized wall shear stress profile of DNS data [5] and current study for case C3

Table 6- Comparison of drag reduction prediction with lower $\boldsymbol{\beta}$ value at $\boldsymbol{Re_\tau = 180}$

Case	Rheological properties			Drag reduction	
	β	Wi_τ	L^2	DNS	current study
D1	0.6	54	100	26	30
D2	0.6	54	1000	61	22
D3	0.6	72	1000	66	28
D4	0.8	54	1000	33	29
D5	0.4	54	1000	64	12

As mentioned above, DNS data shows that by decreasing the value of β or increasing the value of L^2 the DR value increase, but Masoudian et al.'s model [14] cannot predict these trends simultaneously. Therefore, in order to achieve acceptable results in lower β values, the value of L^2 should be small. Case D1 confirms this theory. Moreover in case D4, the value of β is more close to original $\beta = 0.9$ which the turbulence model was developed and consequently the amount of predicted drag reduction in this case is more accurate than the others. In order to investigate Masoudian et al.'s turbulence model [14] with lower β values in more detail, velocity and wall shear stress profiles for case D1 and D4 are shown in Fig. 7 and Fig. 8, respectively.

Results of Fig. 7 show that trends of the DNS data are successfully predicted for velocity profile at both cases (D1 and D4) by Masoudian et al.'s Model [14].

However, predicted values of dimensionless velocity differ slightly from DNS data in the whole channel height.

Based on Fig. 8a viscous shear stress profile is in good agreement with DNS data for case D1. But prediction of polymer shear stress is inconsistent with the DNS data especially near the wall. This may be related to the higher polymer to solvent viscosity ratio (lower β value) than the original one that the turbulence model was developed by Masoudian et al. [14]. In turbulent shear stress profile, although the trends of DNS data and current study are the same but in region where $y^+ > 100$, values of turbulent shear stress are completely incorrect as are predicted higher than the theory line. According to theory, not only components of total shear stress should be below the theory line but also sum of all components should be below the theory line [5].

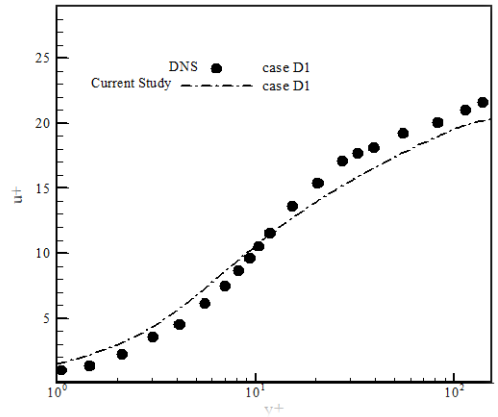

Figure 7- Normalized wall shear stress profile for DNS data [3] and current study in case D1 (a) and D4 (a)

Based on Fig. 8a viscous shear stress profile is in good agreement with DNS data for case D1. But prediction of polymer shear stress is inconsistent with the DNS data especially near the wall. This may be related to the higher polymer to solvent viscosity ratio (lower β value) than the original one that the turbulence model was developed by Masoudian et al. [14]. In turbulent shear stress profile, although the trends of DNS data and current study are the same but in region where $y^+ > 100$, values of turbulent shear stress are completely incorrect as are predicted higher than the theory line. According to theory, not only components of total shear stress should be below the

Theory line but also sum of all components should be below the theory line [5].

Figure 7- Normalized wall shear stress profile for DNS data [3] and current study in case D1 (a) and D4 (b)

Unlike the results of case D1, Fig. 8b shows that polymer and viscous shear stresses are predicted well especially near the wall for case D4. This may be due to the higher value of β ($\beta = 0.8$) in this case. However, as it is seen in case D4, turbulent shear stress values are predicted higher than theory line which is completely wrong. It seems that Masoudian et al.'s turbulence model [14] could not predict eddy viscosity in low β values appropriately. According to Eq. (14) one of the ways to decrease turbulent shear stress is to decrease the value of c_μ . In order to improve the accuracy of the model, the value of c_μ was changed from 0.22 to 0.16.

Fig. 9 shows shear stresses profiles for case D4 after applying this change. Based on this figure, although prediction of turbulent shear stress has been improved, but polymer and viscous shear stresses show more difference with DNS data near the wall in comparison to the original case with $c_\mu = 0.22$. Therefore it seems that improving Masoudian et al.'s turbulence model [14] at lower β values needs more investigations.

5. Conclusion

In present study we examined one of the newest RANS models for viscoelastic fluids described by FENE-P constitutive equation. This model is based on the $k - \epsilon - \overline{v^2} - f$ model which was firstly introduced for Newtonian fluids. In order to study the performance of this turbulence model, several cases with different flow and rheological parameters were investigated. Analysis of the DNS data and the results of current study showed that:

1. Accuracy of the model in prediction of DR value, velocity profile and wall shear stress components is fairly acceptable in many cases especially in high and moderate Reynolds numbers.

2. In low Reynolds numbers (e.g. $Re_\tau = 125$), the value of L^2 plays an important role in the accuracy of

the model. The results with lower value of L^2were more accurate.

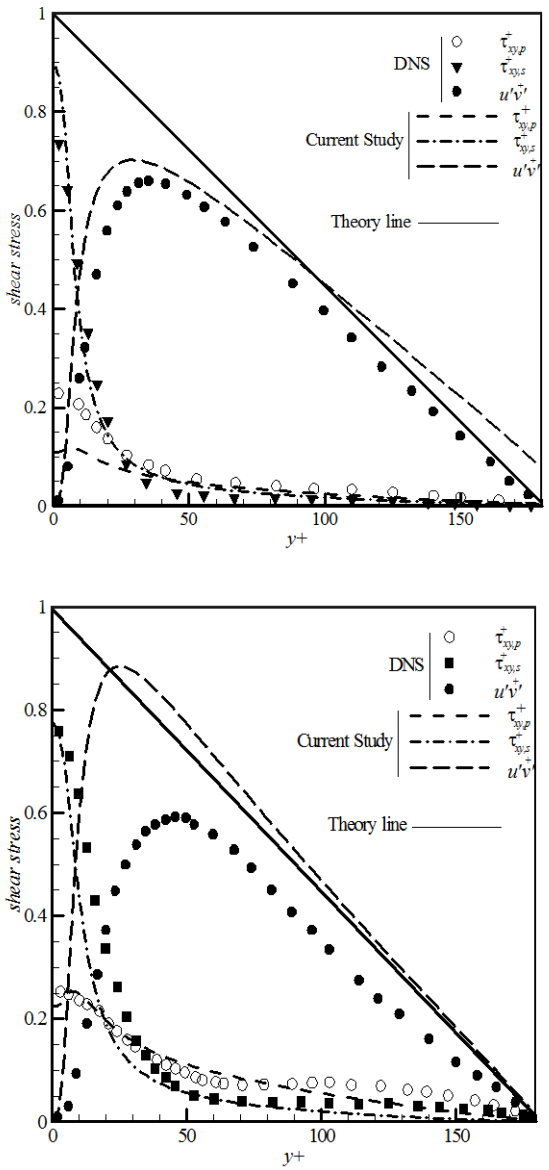

Figure 8- Normalized wall shear stress profile for DNS data [3] and current study in case D1 (a) and D4 (a)

3. In high polymer to solvent viscosity ratio (low β value), not only the model could not predict DR value well, but also it was not able to follow trends of increasing DR value while decreasing β and increasing L^2 based on the DNS data. Also the model could not predict the value of shear stresses correctly, but the trends of wall shear stresses are comparable with the DNS data. Changing the value of c_μ could not improve the accuracy of model significantly therefore in order to improve this turbulence model at lower β values, more investigations should be considered.

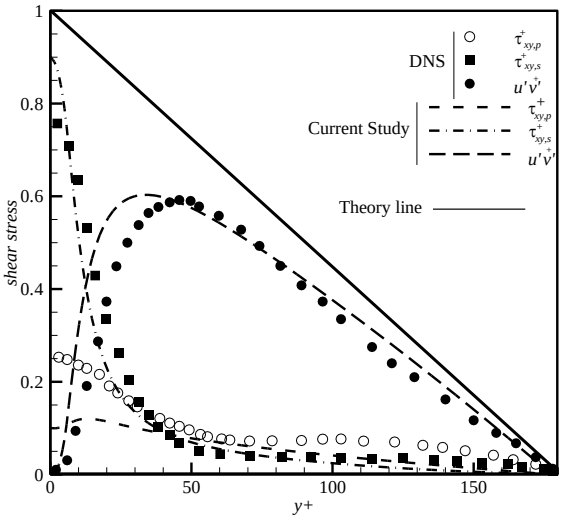

Figure 9- Normalized wall shear stress profile for DNS data [3] and current study with $c_\mu = 0.16$ for case D4

6. References

[1] Virk P. S., 1975, Drag reduction fundamentals, AIChE Journal, 21(4): 625-656.

[2] White C. M., Mungal M. G., 2008, Mechanics and prediction of turbulent drag reduction with polymer additives, Annu. Rev. Fluid Mech 40: 235-256.

[3] Ptasinski P. K., Boersma B.J., Nieuwstadt F. T. M., Hulsen M.A., Van den Brule B. H. A. A., Hunt J. C. R., 2003, Turbulent channel flow near maximum drag reduction: simulations, experiments and mechanisms, Journal of Fluid Mechanics 490: 251-291.

[4] Min T., Yoo J. Y., Choi H., Joseph D. D., 2003, Drag reduction by polymer additives in a turbulent channel flow, Journal of Fluid Mechanics 486: 213-238.

[5] Li C. F., Sureshkumar R., Khomami B., 2006, Influence of rheological parameters on polymer induced turbulent drag reduction, Journal of Non-Newtonian Fluid Mechanics 140(1): 23-40.

[6] Thais L., Gatski T. B., Mompean G., 2012, Some dynamical features of the turbulent flow of a viscoelastic fluid for reduced drag, Journal of Turbulence 13(19): 1-26.

[7] Thais L., Gatski T.B., Mompean G., 2013, Analysis of polymer drag reduction mechanisms from energy budgets, International Journal of Heat and Fluid Flow 43: 52-61.

[8] Pinho F.T., 2003, A GNF framework for turbulent flow models of drag reducing fluids and proposal for a k–ε type closure, Journal of Non-Newtonian Fluid Mechanics 114(2): 149-184.

[9] Pinho F. T., Li, C. F., Younis B. A., Sureshkumar R., 2008, A low Reynolds number turbulence closure for viscoelastic fluids, Journal of Non-Newtonian Fluid Mechanics 154(2): 89-108.

[10] Resende P. R., Pinho F. T., Younis B. A., Kim K.,

Sureshkumar R., 2013, Development of a Low-Reynolds-number k-ω Model for FENE-P Fluids, Flow, turbulence and combustion 90(1): 69-94.

[11] Iaccarino G., Shaqfeh E. S., Dubief Y., 2010, Reynolds-averaged modeling of polymer drag reduction in turbulent flows, Journal of Non-Newtonian Fluid Mechanics 165(7): 376-384.

[12] Thais L., Tejada-Martinez A. E., Gatski T. B., Mompean G., 2010, Temporal large eddy simulations of turbulent viscoelastic drag reduction flows. Physics of Fluids *22*(1): 013103.

[13] Durbin P. A., 1995, Separated flow computations with the k-epsilon-v-squared model, AIAA journal 33(4): 659-664.

[14] Masoudian M., Kim K., Pinho F.T., Sureshkumar R., 2013, A viscoelastic turbulent flow model valid up to the maximum drag reduction limit, Journal of Non-Newtonian Fluid Mechanics 202: 99-111.

[15] Bird R.B., Curtiss C.F., Amstrong R.C., Hassager O., 1987, Dynamics of Polymeric Fluids, John Wiley & Sons, New York, Second Edition.

[16] Dean R.B., 1978, Reynolds number dependence of skin friction and other bulk flow variables in two-dimensional rectangular duct flow, J. Fluids Eng 100(2): 215-223.